Published in final edited form as:
Eur J Pharm Sci. 2013 June 14; 49(3): 390–399. doi:10.1016/j.ejps.2013.04.011.

Evaluation and Modification of Commercial Dry Powder Inhalers for the Aerosolization of a Submicrometer Excipient Enhanced Growth (EEG) Formulation

Yoen-Ju Son[1], **P. Worth Longest**[1,2], **Geng Tian**[2], and **Michael Hindle**[1,*]

[1]Department of Pharmaceutics, Virginia Commonwealth University, Richmond, VA, USA

[2]Department of Mechanical and Nuclear Engineering, Virginia Commonwealth University, Richmond, VA, USA

Abstract

The aim of this study was to evaluate and modify commercial dry powder inhalers (DPIs) for the aerosolization of a submicrometer excipient enhanced growth (EEG) formulation. The optimized device and formulation combination was then tested in a realistic *in vitro* mouth-throat - tracheobronchial (MT-TB) model. An optimized EEG submicrometer powder formulation, consisting of albuterol sulfate (drug), mannitol (hygroscopic excipient), L-leucine (dispersion enhancer) and poloxamer 188 (surfactant) in a ratio of 30:48:20:2 was prepared using a Büchi Nano spray dryer. The aerosolization performance of the EEG formulation was evaluated with 5 conventional DPIs: Aerolizer, Novolizer, HandiHaler, Exubera and Spiros. To improve powder dispersion, the HandiHaler was modified with novel mouth piece (MP) designs. The aerosol performance of each device was assessed using a next generation impactor (NGI) at airflow rates generating a pressure drop of 4 kPa across the DPI. *In silico* and *in vitro* deposition and hygroscopic growth of formulations was studied using a MT-TB airway geometry model. Both Handihaler and Aerolizer produced high emitted doses (ED) together with a significant submicrometer aerosol fraction. A modified HandiHaler with a MP including a three-dimensional (3D) array of rods (HH-3D) produced a submicrometer particle fraction of 38.8% with a conventional fine particle fraction (% <5μm) of 97.3%. The mass median diameter (MMD) of the aerosol was reduced below 1 μm using this HH-3D DPI. The aerosol generated from the modified HandiHaler increased to micrometer size (2.8 μm) suitable for pulmonary deposition, when exposed to simulated respiratory conditions, with negligible mouth-throat (MT) deposition (2.6 %).

Keywords

excipient enhanced growth (EEG); spray drying; hygroscopic aerosol; dry powder inhaler (DPI); aerosolization

[*]Dr. Michael Hindle, PhD (Corresponding author), Virginia Commonwealth University, 410 N. 12th Street, P.O. Box 980533, Richmond, VA 23298-0533, Phone: (804)-828-6497, Fax: (804)-828-8359, mhindle@vcu.edu.

1. Introduction

The dry powder inhaler (DPI) has become widely known as a very attractive platform for drug delivery by virtue of its propellant-free nature, high patient compliance and improved formulation stability (Ashurst et al., 2000; Sumby et al., 1997; Timsina et al., 1994). The current market for DPIs has over 20 passive and active dispersion devices presently in use, and many devices under development for delivering a variety of therapeutic agents (Ashurst et al., 2000; Islam and Gladki, 2008; Son and McConville, 2008). Conventionally, these DPI devices have been designed for powder formulations containing drug particles in the 2–5 μm range and tailored to maximize respirable (% <5μm) particle generation from the powder formulation (Islam and Cleary, 2012; Son and McConville, 2008). The aerosol performance of a DPI is known to be governed by a combination of factors including the physicochemical properties of the powder formulation, the power-deagglomeration mechanisms used to aerosolize the powders, and the patient's inspiratory effort (Son and McConville, 2008).

While much effort has been expended in designing novel DPIs with efficient powder dispersion mechanisms, these new devices have not dramatically increased drug delivery efficiency to the lung. The lung deposition of aerosolized drug from currently available devices varies from 5% to 40% (Ashurst et al., 2000; Newman and Busse, 2002) with a significant fraction of the drug depositing in the patients mouth-throat (MT) region (about 40–70%) due to incomplete drug detachment from carriers or other particles (i.e., deaggregation) during inhalation (Borgstrom et al., 1994; Brand et al., 2007; Geller et al., 2011; Newman et al., 2000). High MT drug deposition also contributes to the large inter- and intra-subject variability observed in the dose delivered to the lungs for DPIs (Borgstrom et al., 2006).

There has been an increased interest in research focusing on inhaled nanoparticle delivery systems due to advantages of nanoscale particles, such as targeting specific cells/organs and rapid drug absorption due to the small size with a large surface area (Yang et al., 2008). In particular, inhaled nanoparticle delivery systems have high potential to significantly reduce extrathoracic depositional drug losses since particles in the range of 40–900 nm are known to achieve near zero deposition in the MT region (Cheng, 2003; Xi and Longest, 2008). However, nanoparticle delivery to the lungs has many challenges including formulation instability due to particle–particle interactions and poor deposition efficiency due to exhalation of low-inertia nanoparticles (Jaques and Kim, 2000). Attempts to overcome these issues have led to most inhalation dry powder nanoparticle formulations being designed as micron-sized collections of nanoparticles, or aggregated nanoparticles (Yang et al., 2008). However, as the nanoparticles are now presented as conventionally sized inhalation aerosols, most of the potential drug delivery advantages are negated and they have MT deposition losses consistent with conventional inhaled products.

One solution to improve aerosol delivery efficiency and nearly eliminate unwanted extrathoracic aerosol deposition adopts a dynamic aerosol particle size approach rather than the conventional static particle size used for current DPIs. Excipient enhanced growth (EEG) is a newly proposed respiratory delivery strategy which delivers an inhaled submicrometer particle formulation to minimize MT depositional losses. The aerosol increases to micrometer size during inhalation in order to maximize lung retention (Hindle and Longest, 2012; Longest and Hindle, 2011). In the EEG approach, combination drug and hygroscopic excipient dry powder particles are produced in the size range of 100–900 nm in order to minimize MT deposition during inhalation. After bypassing the MT region, the natural humidity in the lungs causes the particles containing the hygroscopic excipient to accumulate water, increasing the size and weight of the particles. The addition of the hygroscopic excipient (eg mannitol) enhances the aerosol particle growth compared to drug

only formulations (Hindle and Longest, 2012). Increasing the aerodynamic particle size to 2–4 μm then ensures near complete lung deposition. In a previous study, (Longest and Hindle, 2011) developed correlations based on an experimentally validated model to predict the size increase of initially submicrometer combination drug and hygroscopic excipient particles in the airways and demonstrated diameter growth ratios of up to 4.6 at excipient mass loadings of 50% and below (Longest and Hindle, 2011). Longest et al., (2012b) also reported less than 1% MT deposition using the EEG application in combination with liquid EEG formulations aerosolized using the Respimat inhaler, based on *in vitro* experiments and computation fluid dynamics (CFD) simulations (Longest et al., 2012b). The development of a submicrometer spray-dried EEG formulation for use in DPI devices was described by Son et al. (Son et al., 2013; Son et al., 2012c). In this previous work, an optimized EEG powder formulation exhibited a fine particle fraction (% <5μm) of 95.3% with negligible *in vitro* MT deposition (4.1%) when aerosolized using the Aerolizer (Son et al., 2012b).

The aim of this study was to evaluate the ability of commercially available and modified DPIs to aerosolize an optimized dry powder formulation to maximize the submicrometer particle fraction for the EEG application. Five active and passive dispersion commercial DPIs were evaluated, along with aerosolizing the formulation using a modified HandiHaler DPI that employed novel mouthpiece (MP) designs and a unique capsule piercing approach. A combination of computational fluid dynamics (CFD) analysis and *in vitro* experiments were employed to develop and evaluate the design modifications to the HandiHaler. Performance of the optimal DPI is then evaluated in a geometrically realistic MT and lung model in terms of extrathoracic deposition and aerosol size increase over an inhalation cycle time period using both CFD simulations and *in vitro* experiments. Previous studies using this model have shown a good in vitro-in vivo correlation of MT deposition (Delvadia et al., 2012)

2. Materials and Methods

2.1. Materials

Albuterol sulfate (AS) USP was purchased from Spectrum Chemical Co. (Gardena, CA). Pearlitol® PF-Mannitol was donated from Roquette Pharma (Lestrem, France). Poloxamer 188 (Leutrol F68) was donated from BASF Corporation (Florham Park, NJ). L-leucine and all other reagents were purchased from Sigma Chemical Co. (St. Louis, MO). Size 3 hydroxypropylmethyl cellulose (HPMC) capsules were donated from Capsugel (Morristown, NJ). The following DPIs were employed in this study: Aerolizer® (Novartis; Basel, Switzerland), HandiHaler® (Boehringer Ingelheim GmbH; Rhein, Germany), Novolizer® (Meda Pharma; Bruxelles, Belgium), Exubera® (Pfizer; New York, NY) and Spiros® (Dura Pharmaceuticals; San Diego, CA). A Vortex® non-electrostatic holding chamber was purchased from PARI Respiratory Equipment, Inc. (Midlothian, VA). Molykote®316 silicone release spray was purchased from Dow Corning Corporation (Midland, MI).

2.2. Preparation of spray-dried EEG particles

A dry powder EEG formulation consisting of AS (drug), mannitol (hygroscopic excipient), L-leucine (dispersion enhancer) and poloxamer 188 (surfactant) in a ratio of 30:48:20:2 %w/w, was prepared by spray drying using a Büchi Nano spray dryer B-90 (Büchi Laboratory-Techniques, Flawil, Switzerland). The spray feed solution for spray-drying was prepared by addition of 75 mg of AS, 120 mg of mannitol, 50 mg of L-leucine and 5 mg of poloxamer to 80:20% v/v water:ethanol solution (50 mL) (Son et al., 2013; Son et al., 2012c). The following conditions were used during spray drying: drying airflow, 120 L/min; liquid feed rate, 100%; spray nozzle, vibrating mesh nozzle; nozzle cap size, 4μm. The inlet temperature

was established at 70 °C and the outlet temperature was 45 °C. The dried solid particles were collected from an electrostatic precipitator and stored in sealed capped amber vials. The vials containing powders were stored in a desiccator (approximate RH <10%) at room temperature.

AS drug content uniformity of the formulations was determined using a validated HPLC method (see Section 2.6). Briefly, a solution of each sample was prepared by dissolving approximately 3 mg of powder, which was accurately weighed, in 10 mL of deionized water. This solution was then injected directly into the HPLC for quantification.

2.3. Aerodynamic particle size characterization

A Next Generation Impactor (NGI; MSP Corp., Shoreview, MN) was used to determine aerodynamic particle size characteristics of the drug when aerosolized using the DPIs. For the passive DPIs (Aerolizer, Novolizer and HandiHaler) the devices were actuated at flow rates of 80, 80 and 45 L/min, respectively. The air flow rates were selected to generate a pressure drop of 4 kPa across the DPIs except for Aerolizer, which was tested at 80 L/min due to vacuum pump flow limitations. For the active dispersion DPIs, Exubera and Spiros, each was actuated at a flow rate of 30 L/min. For each device, 2 mg of formulation was loaded into the DPI. The inhalers were actuated by drawing air through the inhalers at the flow rates described above. The simulated inhalation time was varied depending on the flow rate in order to pull at total volume of 4L of air through each DPI at ambient conditions (22–25 °C / 45–55% RH). Each measurement was repeated three times. All DPIs were actuated in a horizontal position and the aerosol output was delivered to the NGI for particle sizing via the pre-separator. In order to assess the particle size distribution of the total aerosol, the USP induction port was omitted. For each of the impactor experiments, the impactor collection stages and pre-separator were coated with silicone spray to minimize particle re-entrainment and bounce (Akihiko et al., 2004). AS remaining in the DPI (where possible to recover), deposited on the pre-separator, and on each of the impactor collections stages was recovered by washing with a suitable volume of deionized water to extract the drug for quantitative analysis. Collected samples were analyzed using a validated HPLC method (Section 2.6).

Drug emitted dose (ED), defined as the percent of AS exiting the DPI, was determined by subtracting the amount of AS remaining in the DPI from the initial mass of AS loaded. The initial mass loaded in the DPI was calculated from weight of combination formulation and the measured % AS content for each formulation. The drug fine particle fraction ($FPF_{5\mu m/ED}$) and submicrometer particle fraction ($FPF_{1\mu m/ED}$) were defined as the percentage of the emitted dose of AS with aerodynamic diameters smaller than 5 μm and 1 μm, respectively. These were calculated via interpolation of the % mass less than 5 μm and 1 μm, respectively, on a plot of the cumulative percentage mass verses cutoff diameter of the respective stages of the NGI. The MMAD was determined at the 50^{th} percentile on the % cumulative undersize (probability scale) versus logarithmic aerodynamic diameter plot. The mass median diameter (MMD) of aerosol was derived from the MMAD and skeletal density (ρ) (Son et al., 2012b) according to Eq. (1).

$$MMD = \frac{MMAD}{\sqrt{\rho}} \quad (1)$$

2.4. HandiHaler Modifications

In order to improve the HandiHaler powder dispersion characteristics, modifications were made to reduce the capsule aperture dimensions and with the addition of a secondary

dispersion zone within the inhaler mouthpiece. Capsules with two 0.5 mm pre-pierced holes (HH-CAP) were tested compared to the 1.5 mm holes generated by the Handihaler piercing mechanism. Hole position on the capsule was maintained through the tests and a flow rate of 45 L/min was employed to actuate the inhaler. Two designs of the secondary dispersion zones were evaluated, a mouthpiece with a two-dimensional mesh (HH-2D), and a mouthpiece with a three-dimensional rod array (HH-3D). Both these designs were tested with the 0.5 mm hole pre-pierced capsules. For these experiments, the Handihaler mouthpiece (Figure 1a) was replaced with either the two-dimensional (2D) mesh MP (Figure 1b) or the three-dimensional (3D) rod array MP (Figure 1c) while maintaining the original HandiHaler capsule holding base unit. The MPs were fabricated from polycarbonate resin on rapid prototyping equipment (Viper SLA system, 3D Systems, Valencia, CA). As described previously, each device was loaded with 2 mg of formulation and actuated into the NGI at airflow rates corresponding to a pressure drop of 4 kPa across the DPI. The air flow rates for the HH-2D and HH-3D MPs were 53 and 45 L/min, respectively.

2.5. EEG aerosol characterization in the mouth-throat - tracheobronchial (MT-TB) model using *in vitro* and CFD analysis

The MT deposition and hygroscopic growth of AS in the optimized combination powder formulations were evaluated using *in vitro* deposition experiments in a MT-TB geometry. A schematic diagram of experimental set up for the EEG study is shown in Figure 2. The characteristic airway geometry consisted of a MT and upper TB section through the third respiratory bifurcation (B3). Details of the MT and upper TB components of this model were previously described in the studies of Tian et al. (Tian et al., 2011a; Tian et al., 2011b) and Xi and Longest (2007). The TB region of the model was housed in a chamber designed to provide a residence time of approximately 2 s at 45 L/min and route the aerosol into an impactor for sizing.

The deposition of AS in the MT-TB model and the final drug aerosol particle size exiting the model were assessed following aerosol exposure to simulated airway conditions (37 °C/ 99% RH). To simulate the wet-walled conditions of the respiratory tract, the walls of the MT-TB model housed in the chamber were pre-wetted and the model was placed in an environmental cabinet (Espec; Hudsonville, MI) to maintain a wall temperature of approximately 37°C. The outlet of the model was connected to the NGI which was also housed in the cabinet when the final drug particle size distribution following exposure to humidified conditions was investigated. In order to actuate the DPI outside of the environmental chamber, a small volume spacer (Figure 2) was introduced between the DPI outlet, which remained outside the environmental chamber, and the inlet to the MT-TB model, which was inside the environmental chamber. This was employed due to physical experimental limitations and would not be used by a patient. The initial aerodynamic particle size of the aerosol exiting the spacer was determined using the NGI at ambient conditions. For all runs, the dry powder aerosol was generated using the modified HandiHaler (HH-3D) DPI actuated using external ambient conditions. Each powder formulation (2 mg) was filled into size 3 HPMC capsules and placed into the DPIs prior to testing. The HH-3D device was actuated using an air flow rate of 45 L/min for 5 seconds. Drug aerosol deposition in the MT and TB regions of the model and on each impactor stage was determined by washing each deposition site with 10 mL of deionized water. The collected samples were analyzed using a validated HPLC method (Section 2.6).

A numerical mesh of the airway geometry was constructed for CFD simulations using hexahedral elements to the extent possible, as specified by Vinchurkar and Longest (Vinchurkar and Longest, 2008). Hexahedral mesh elements were used exclusively in the MT and TB regions of the model and multiple rows of hexahedral elements were used on the inner chamber surfaces where deposition may occur. However, due to the complexity of

the geometry, some tetrahedral elements were required to fill the chamber area and create a continuous field. Final meshes of the MT-TB geometry and chamber contained 761,259 and 729,180 control volumes, respectively. Near-wall grid spacing of the MT-TB geometry and chamber was maintained to be less than 0.8 and 1.2 mm, respectively. Comparison with a grid containing approximately 1.5 times more control volumes produced less than 3% relative difference in maximum velocity, outlet aerosol size, and particle deposition fractions.

Computational fluid dynamics simulations of fluid flow, heat and mass transport, along with droplet trajectories, size change, and deposition were considered using a combination of a commercial code (Fluent 12, Ansys Inc.) and user-supplied routines. To effectively address both laminar and turbulent flow conditions, a low Reynolds number (LRN) k-ω turbulence model was selected. This model has previously been well tested, and found to provide good estimates of aerosol transport and deposition in upper airway geometries (Longest and Vinchurkar, 2007; Xi et al., 2008). To evaluate the variable temperature and RH fields in the MT-TB model, interconnected relations governing the transport of heat and mass (water vapor) were also included. These governing equations were previously presented in detail by Longest and Xi (2008) and Longest et al., (2007).

To simulate droplet trajectories, including hygroscopic size change, a Lagrangian model was implemented that accounted for drag, gravitational, and Brownian motion effects as previously described in the study of Longest and Hindle (2010). To model the effect of turbulent fluctuations on droplet trajectories, or turbulent dispersion, a random walk method was implemented that included a previously described correction for near-wall anisotropic turbulence (Longest et al., 2007). Deposition predictions of this model were previously shown to agree well with *in vitro* experiments for ambient aerosols, pharmaceutical sprays, and powders delivered from inhalers (Hindle and Longest, 2012; Longest and Hindle, 2009; Longest et al., 2007; Longest et al., 2008; Longest et al., 2012c; Tian et al., 2011b).

The droplet evaporation and condensation model employed in this study was similar to previous approximations for salts (Ferron, 1977; Ferron et al., 1988; Hinds, 1999) and multicomponent aerosols (Longest and Hindle, 2010). The heat and mass transfer relations for multicomponent hygroscopic droplets in the respiratory airways were previously reported by Longest and Xi (2008). This model employs a rapid mixing approach, which assumes conditions inside the droplet are constant and gradients are negligible compared with gradients in the air phase. The droplet model accounts for interdependent heat and mass transfer, which results in droplet heating during condensation and cooling during evaporation as a function of the surrounding temperature. Mass and heat fluxes at the droplet surface are modified for non-continuum effects using the Knudsen correlation (Finlay, 2001). Blowing velocity effects were also considered (Longest and Xi, 2008). For multicomponent droplets containing water, drug, and hygroscopic excipient, properties along with hygroscopic effects and the Kelvin effect were previously described by Longest and Hindle and are incorporated into this study (Longest and Hindle, 2011; Longest and Hindle, 2012).

A user routine was employed to model interconnected droplet temperature and size change resulting from condensation and evaporation. This droplet model accounts for the Kelvin effect, hygroscopicity arising from the dissolved drug and excipient, and the effect of droplet temperature on surface vapor pressure. In simulating aerosol evaporation and growth, the effect of the droplets on the continuous phase was neglected, resulting in a one-way coupled approach. One-way coupled simulations are expected to be accurate in this study due to the presence of wetted walls.

Boundary conditions of the numerical model included walls saturated with water vapor and maintained at 37 °C to match the *in vitro* experiments. Inlet air conditions matched the ambient experimental conditions (21 °C and 40% RH) and included steady state flow through the model at 45 LPM.

In performing the CFD simulations, previously established best-practices were implemented to provide a high quality solution. All transport equations were discretized to be at least second order accurate. Convergence of the flow field solution was assumed when the global mass residual had been reduced from its original value by five orders of magnitude and when the residual-reduction-rates for both mass and momentum were sufficiently small. To improve accuracy and to better resolve the significant change in flow scales during deposition, all calculations were performed in double precision. In order to produce convergent deposition results, 90,000 initial droplets were released for each of the cases considered. Mass median aerodynamic diameters after growth were calculated based on the NGI stage midpoint diameters. Doubling the number of droplets considered had a negligible impact on both total and sectional deposition results.

2.6. High-performance liquid chromatography (HPLC)

AS quantification was performed using a validated HPLC method. A Waters 2690 separations module with a 2996 PDA detector (Waters Co., Milford, MA) was used. Chromatography was performed using a Restek Allure PFP 15 × 3.2 mm column (Bellefonte, PA). The mobile phase, consisting of methanol and ammonium formate buffer (20 mM, pH 3.4) in a ratio of 70:30, respectively, was eluted at a flow rate of 0.75 mL/min and the UV detector was set to a wavelength 276 nm. The column temperature was maintained at 25 °C, and the volume of each sample injected was 50 μL.

2.7. Statistical analysis

Data were expressed as the mean plus/minus standard deviation (SD). Statistical differences were studied by either analysis of variance or student's t-test using Jump 9.0 software (SAS Institute Inc., Cary, NC). *P* values of less than 0.05 were considered as statistically significant. To identify the statistically significant effect of DPI devices on the aerosolization properties of EEG formulation, one-way analysis of variance (one-way ANOVA) followed by post hoc Dunnett's test with a control was used. The significance level was 0.05.

3. Results and Discussion

3.1. Effect of DPI on the aerosolization of EEG formulation

In this study, five conventional DPI devices were evaluated for their ability to effectively aerosolize a carrier-free EEG dry powder formulation and produce a high submicrometer particle fraction. It is important to recognize that DPI performance is significantly dependent upon the powder formulation to be aerosolized. For these studies, we have developed a spray dried submicrometer powder formulation which has been previously described (Son et al., 2013; Son et al., 2012c). The powder formulation containing drug and hygroscopic excipients was engineered to combine the high MT penetration efficiency of submicrometer aerosol particles with the lung deposition efficiency of micrometer sized particles by utilizing hygroscopic growth during the inhalation cycle. The optimized EEG powder formulation was produced using the following conditions: 0.5% w/v solids concentration, consisting of AS, mannitol, leucine and poloxamer in a ratio of 30/48/20/2, respectively in a water:ethanol (80:20 % v/v) solution which was spray dried using the 90 cm drying chamber and 4 μm spray mesh at 70°C (Son et al., 2013; Son et al., 2012c). Figure 3 shows a

scanning electron micrograph of a typical formulation, spherical discrete submicrometer particles were observed.

The DPIs used in this study (except Exubera) were originally designed to aerosolize carrier-based formulations, thus the powder dispersion mechanism for such DPIs was optimized to maximize micronized drug detachment from carrier particles utilizing a impaction grids (Aerolizer), impaction/turbulence (HandiHaler), a cyclone (Novolizer) and rotating impellers (Spiros) (Islam and Cleary, 2012; Smith and Parry-Billings, 2003; Son and McConville, 2008). Unlike the DPIs listed above, Exubera was designed to aerosolize carrier-free spray dried combination powder using a fixed volume of compressed air (Harper et al., 2007; Son and McConville, 2008).

Table 1 shows the aerosolization characteristics of the optimized EEG formulation in the conventional active and passive DPIs. For this formulation, it has been previously shown that most primary particles were in the submicrometer size range (Son et al., 2013). Therefore, the aerosolization results indicate the relative efficiency of the DPIs to disperse the formulation to primary particles for inhalation. Overall, the DPIs exhibited excellent aerosolization of the carrier-free submicrometer particles with greater than 80% of $FPF_{5\mu m/ED}$, which is much higher than the previously reported values for these DPI when aerosolizing conventional formulations (15–50%) (Dolovich, 1999; Fenton et al., 2003; Harper et al., 2007; Smith and Parry-Billings, 2003; Srichana et al., 1998), due to combined effects of the submicrometer primary particle size and the powder formulation excipients. There were significant differences in the ED (P=0.0262), MMAD (P<0.0001), $FPF_{5\mu m/ED}$ (P<0.0001) and submicrometer fraction ($FPF_{1\mu m/ED}$) (P<0.0001), indicating differences in the powder deagglomeration performance among the DPIs.

The active dispersion DPIs, Exubera and Spiros, were observed to be non-optimal for dispersing the EEG formulation into primary particles. This is unexpected because these devices are considered to be the most innovative with reported high dispersion efficiency and flow-rate independent performance (Dolovich, 1999; Harper et al., 2007; Son and McConville, 2008). Emitted doses (ED) for the two active devices were observed to be the lowest, with the Spiros and Exubera DPIs producing MMADs of 2.6 and 2.0 μm, respectively. For these inhalers, the $FPF_{1\mu m/ED}$ was less than 10% of the emitted dose. This was particularly surprising for Exubera, which was expected to be an ideal dispersion device for the EEG formulation due to the similarities in dose (1–3 mg), formulation design (carrier-free spray dried powders) and excipients (mannitol and amino-acid) (Harper et al., 2007). Possible explanations for this low dispersion efficiency of the submicrometer particles may included the fact that the volume of compressed air (about 8 mL) supplied to the formulation, which is the main dispersion energy source, was optimized to generate aerosols in the micrometer size range (Harper et al., 2007). It was also observed that the large holding chamber had significant drug retention (> 35% of the loaded dose), which has also been observed in other studies, resulting in a relatively low emitted dose (Harper et al., 2007).

The capsule-based passive DPIs, Aerolizer and Handihaler, showed better submicrometer particle generation with smaller MMAD than other DPIs tested in this study (Table 1). As previously reported, the Aerolizer operating at 80 L/min was capable of producing an aerosol with a high emitted (81.4%) and submicrometer dose fraction (28.3%). In comparison, the HandiHaler operating at 45 L/min had a similar emitted dose (Dunnett's method: P=0.1427), and MMAD (Dunnett's method: P=0.0552) compared to the Aerolizer. The $FPF_{1\mu m/ED}$ for HandiHaler was 19.5%, indicating significantly decreased dispersion efficiency of primary submicrometer particles compared to Aerolizer (Dunnett's method: P=0.0036).

The primary forces leading to powder deagglomeration in DPIs are known to be turbulence, mechanical forces, such as impaction and vibration, or combinations of both (Voss and Finlay, 2002). For the capsule based systems, besides the forces listed above, shear force created when powder agglomerates are released through the small holes in the capsule are also know to have significant contribution to powder deagglomeration. Studies by Coates et al., (2005) and Chew et al., (2002) demonstrated that *in vitro* aerosol performance improved with decreased capsule aperture size due to the higher dispersion energy generated by smaller aperture on the capsule (Chew et al., 2002; Coates et al., 2005). The improved submicrometer aerosol particle generation observed with the Aerolizer compared to HandiHaler may be due to the smaller aperture size (0.5 mm vs 1.5 mm, respectively) providing higher shear forces to the powder aggregates during capsule emptying.

3.2. Modification of HandiHaler

In the next stage of the study, the HandiHaler DPI was considered for device modification in an attempt to maximize submicrometer aerosol generation during aerosolization. It was noted that the aerosolization performance of the HandiHaler was similar to the Aerolizer, but at a lower inhaled flow rate. A low inhaled flow rate may be advantageous for DPI delivery since drug deposition in the extrathoracic airways by inertial impaction can be minimized. It is also recognized that mouth-throat deposition is strongly related to the velocity of air flow exiting the device. Generally, an increased air flow rate increases the mouth-throat deposition (DeHaan and Finlay, 2004; Grgic et al., 2004).

In this study, the first modification was made to the capsule. It is known that the aperture size of the capsule has significant effects on the inhaler performance since the capsule can provide additional deagglomeration dependent on the size of the capsule hole (Chew et al., 2002; Coates et al., 2005). The HandiHaler was primed by piercing a loaded capsule with HandiHaler needles which produced two 1.5 mm diameter holes on the side of capsule. In order to make smaller holes, a 25G needle was used to pierce the capsule to produce two 0.5 mm holes. The powder dispersion properties of two setups, 1.5 mm holes vs. 0.5 mm holes, were compared to evaluate the influence of aperture size on the powder dispersion with the HandiHaler. Table 2 indicates significant increase in the $FPF_{5\mu m/ED}$ (Dunnett's method: P=0.0056) and reduction in the MMAD (Dunnett's method: P=0.0359) for the 0.5 mm hole setup with a similar ED (Dunnett's method: P>0.05) compared to 1.5 mm holes. However, the $FPF_{1\mu m/ED}$ was not significantly improved (Dunnett's method: P>0.05). This result indicates that decreasing the capsule aperture size may have improved break-up of large agglomerates. However, increasing the shear force by modifying the capsule aperture size was not sufficient to completely deagglomerate submicrometer particles with high inter-particle forces.

The second modification was made to the mouthpiece (MP) flow passage of the DPI. The geometry and length of the device MP are key DPI design parameters, which will influence the effective dispersion of drug powder formulations (Coates et al., 2007). Several studies have demonstrated that the geometry of a DPI MP can have significant effects on performance, including altering the turbulence kinetic energy generated and the amount of drug deposition in the MT region during *in vitro* testing (Coates et al., 2007; DeHaan and Finlay, 2004; Grgic et al., 2004). Figures 1b and 1c show the two new MP designs containing a 2D mesh (HH-2D) and 3D rod array (HH-3D) that were fabricated, respectively. These designs were connected to the HandiHaler capsule base unit to evaluate their effects on powder deagglomeration performance and compared with the commercial Handihaler MP (Figure 1a). In an attempt to maximize the dispersion efficiency, the novel MP designs were tested with capsule pierced with the 0.5 mm hole size. Table 2 shows that the aerosolization performance of the 2D mesh (HH-2D) and 3D rod array (HH-3D). In the case of HH-2D, there was no significant change in the ED or $FPF_{1\mu m/ED}$ compared to HH;

however, the $FPF_{5\mu m/ED}$ was increased. For the HH-3D design, compared to HH, there was an increase in both $FPF_{5\mu m/ED}$ (Dunnett's method: P=0.0007) and $FPF_{1\mu m/ED}$ (Dunnett's method: P=0.0007), while the overall aerosol MMAD was reduced (Dunnett's method: P=0.0001) at a constant pressure drop of 4 kPa. The calculated mass median diameter (MMD) of the aerosol for the HH-3D was 0.98 μm. Furthermore, it should be noted that these changes did not significantly alter the ED (Dunnett's method: P>0.05) which was 74.2%, suggesting no significant change in device retention when compared to HH.

In a companion study, Longest et al., 2013 explored the mechanisms of powder deaggregation in carrier-free capsule-based inhalers. Considering a range of MP flow passage designs and flow rates, Longest et al., 2013 determined that for a carrier-free formulation, a new parameter defined as the non-dimensional specific dissipation (NDSD) best correlated with aerosol deaggregation in terms of $FPF_{1\mu m}$, MMD, and MMAD. This new parameter captures the effects of turbulence, eddy length scale, and particle exposure time to turbulence. The NDSD highlights that the most effective deaggregation is achieved when high turbulent energy occurs in small eddies with extended particle residence times. In contrast, the previously proposed integral shear strain rate (ISSR) (Coates et al., 2004) is based on particle interactions with large integral scale eddies. Across a range of deaggregation designs (constriction tube, impaction baffle, inward jets, 2D mesh, 3D mesh, and 3D rod array) for a variety of flow rates and pressure drops, the NDSD parameter best correlated with aerosol MMD with a correlation coefficient of $R^2 = 0.8$.

For the three MPs considered in the current study, 3D contour plots of the NDSD parameter are shown in Figure 4. Flow rates for the constriction tube, 2D mesh, and 3D rod array were consistent with a pressure drop of 4 kPa, resulting in simulated values 45, 53, and 45 L/min, respectively. The 2D mesh design is observed to increase the NDSD parameter through the center of the flow stream where interactions with particles are expected to be the largest, compared with the constricted tube design of the HandiHaler. However, the region of NDSD increase is limited to the vicinity of the mesh for the 2D design. In contrast, the 3D rod array increases both the magnitude of the NDSD parameter and the extent of elevated values. Both volume-averaged values of NDSD in the mouthpiece flow passage and the resulting experimentally measured MMD are reported in Figure 4 and Table 2. Volume-averaged NDSD values are similar between the HH MP and 2D mesh designs, which is consistent with the similar resulting MMDs (1.3 μm vs. 1.24 μm). In contrast, the NDSD parameter in the 3D rod array design is twice as large as with the other two models. This large increase in NDSD corresponds to the significantly smaller MMD observed with the 3D rod array (0.98 μm). As a result, a qualitative association is demonstrated in this study between increasing NDSD and reduced MMD. Furthermore, the improved performance of the 3D rod array may be due to the parameters captured by the NDSD, with increased deaggregation correlating directly with increased turbulence strength, reduced eddy size, and increased exposure time to turbulence. Longest et al., 2013 demonstrated that for a carrier-free system with either the 2D mesh or 3D rod array designs, particle-wall interactions did not correlate with aerosol deaggregation.

3.3. EEG aerosol characterization in the MT- TB model using *in vitro* and CFD analysis

The EEG combination particle formulation was aerosolized using the HH-3D inhaler at 45 L/min in the MT-TB with simulated airway conditions to evaluate the effects of EEG on the (i) MT deposition and (ii) the final particle size exiting the model. The HH-3D device was selected as it performed best in terms of aerosolization among the conventional and modified DPIs that had been tested. A realistic MT-TB model designed by Xi and Longest (2007) was used to evaluate the AS MT deposition of the EEG combination particles. Previous studies using this model had shown a good *in vitro-in vivo* correlation of MT deposition (Delvadia et al., 2012).

Table 3 shows that the MT deposition of EEG particles aerosolized using the modified HandiHaler (HH-3D) was 2.6% of the emitted dose using simulated airway conditions, which was a significant improvement over 50–60% drug MT deposition observed by Delvadia et al., (2012) using flow rates between 65–99 L/min with a carrier-based Budelin Novolizer (Delvadia et al., 2012) when tested using the same experimental set up. Deposition of the EEG aerosol in the TB regions of the model (generations 1–3) was also low. The low drug deposition in the MT region was mainly due to the generation of a highly dispersible submicrometer aerosol which was able to penetrate this region of the extrathoracic airways. Based on *in vitro* experiments with the MT-TB model, about 97% of emitted particles successfully bypassed MT-TB passages with less than about 3% depositing by inertial impaction, which offers an order of magnitude improvement compared to the MT deposition commonly observed with commercial DPIs.

In order for the EEG concept to be feasible, following inhalation the submicrometer particles must increase in size to enable deposition within the airways, rather than being exhaled. Table 3 shows the final MMAD of the aerosol following passage through the MT-TB model and chamber with the simulated airway humidified conditions was 2.8 μm with a submicrometer fraction ($FPF_{1\mu m/ED}$) of only 3%. This provides evidence that the submicrometer combination particles grew to a size suitable for lung deposition due to the hygroscopic nature of the particles and their interaction with the simulated airway relative humidity. For these experiments which employed the spacer chamber to link the DPI at ambient conditions with the MT-TB model housed in the environmental chamber, the initial aerosol mean (SD) MMAD was 1.3 (0.1) μm and the submicrometer fraction ($FPF_{1\mu m/ED}$) was 31.7 (1.6) % when the formulation was aerosolized under ambient conditions. Experimentally the spacer chamber was necessary to physically connect the DPI and the model. This allowed for the DPI to be actuated using ambient air and to protect it from the temperature and humidity conditions in the environmental cabinet.

CFD simulations were employed to visualize the aerosol growth process and to compare the aerosol generation in the presence and absence of the spacer chamber, in order to assess its effects on the MT deposition and final MMAD. Figures 5a and b show the predicted velocity profiles with (same as the experimental set up) and without the spacer, respectively. The presence of the spacer appears to reduce the velocity within the mouth region compared with when the DPI is actuated directly into the mouth at 45 L/min. Similarly in Figures 6a and b, which show the predicted RH contours within the airway geometry with and without the spacer, respectively, removing the spacer produces higher gradients in the flow field of RH contours. Furthermore, introducing the powder aerosol directly into the mouth appeared to produce lower RH within the mouth compared to using the spacer. Figures 7a and b show the particle growth trajectories with and without the spacer, respectively. The predicted final particle sizes were similar, suggesting that the use of the spacer did not have a significant effect on aerosol growth characteristics. In addition, the predicted value for the final aerosol size of 2.71 μm agreed well with the experimental value of 2.8 μm.

The EEG aerosol formulation increased to micrometer size when the submicrometer primary particles, which were efficiently aerosolized using an optimized DPI, were exposed to a simulated *in vitro* airway model. Aerosol particle growth took place over a 2 s inhalation period to produce a final aerosol size that would be suitable for airway deposition with minimal MT loses. Table 3 shows that the final $FPF_{5\mu m/ED}$ value was over 75% of the emitted dose, which is significantly better than typically observed for conventional inhaled DPI products. Newman et al. (2000) showed 25% budesonide deposition in the Lung at 60 L/min with a Novolizer DPI (Newman et al., 2000); Brand et al. (2007) showed 18% tiotropium bromide deposition with a HandiHaler DPI (Brand et al., 2007); and the novel

PulmoSphere formulation, carrier-free low particle density spray dried powder, exhibited 34.2% tobramycin lung deposition with a matched T-326 inhaler (Geller et al., 2011).

In addition to low MT deposition and increase to conventional aerosol size, delivery of EEG aerosols may have advantages in terms of targeting deposition to different regions of the airways. A recent CFD study by Tian et al. (2012) demonstrated that with the EEG approach regional lung deposition in the lower TB airways, which are largely affected by lung diseases, could be increased by a factor of 20–30× compared with conventional inhalation delivery. With a quick and deep inhalation profile, predictions indicated that 90% drug delivery to the alveolar region was possible with EEG aerosols.

4. Conclusion

Spray dried combination drug and excipient particles were produced with a submicrometer primary particle size suitable for use in the EEG application. The device-EEG formulation performance was optimized to generate submicrometer primary particles. The combination EEG particles exhibited excellent aerosolization properties with a submicrometer fraction of 38.8% using a modified HandiHaler DPI (HH-3D) at 45 L/min. The submicrometer combination aerosols, when exposed to simulated respiratory conditions, increased to micrometer-size particles suitable for pulmonary deposition with negligible MT loss (2.6%). The excipient enhanced growth (EEG) approach may enable the high efficiency delivery of submicrometer aerosol particles, which will then increase in size within the airways, and result in nearly complete pulmonary deposition with the potential for targeting delivery to different regions of the lungs.

Acknowledgments

This study was supported by Award Number R21 HL104319 and R01 HL107333 from the National Heart, Lung, and Blood Institute. The content is solely the responsibility of the authors and does not necessarily represent the official views of the National Heart, Lung, and Blood Institute or the National Institutes of Health. Microscopy was performed at the VCU Department of Anatomy and Neurobiology Microscopy Facility, supported, in part, with funding from NIH-NINDS Center core grant (5P30NS047463-02).

References

Akihiko K, Sakagami M, Hindle M, Byron PR. Aerodynamic sizing of metered dose inhalers: An evaluation of the andersen and next generation pharmaceutical impactors and their USP methods. J Pharm Sci. 2004; 93:1828–1837. [PubMed: 15176070]

Ashurst I, Malton A, Prime D, Sumby B. Latest advances in the development of dry powder inhalers. Pharm Sci Technol Today. 2000; 3:246–256. [PubMed: 10884680]

Borgstrom L, Bondesson E, Moren F, Trofast E, Newman SP. Lung deposition of budesonide inhaled via Turbuhaler: a comparison with terbutaline sulphate in normal subjects. Eur Respir J. 1994; 7:69–73. [PubMed: 8143834]

Borgstrom L, Olsson B, Thorsson L. Degree of throat deposition can explain the variability in lung deposition of inhaled drugs. J Aerosol Med. 2006; 19:473–483. [PubMed: 17196076]

Brand P, Meyer T, Weuthen T, Timmer W, Berkel E, Wallenstein G, Scheuch G. Lung deposition of radiolabeled tiotropium in healthy subjects and patients with chronic obstructive pulmonary disease. J Clin Pharmacol. 2007; 47:1335–1341. [PubMed: 17625157]

Cheng YS. Aerosol Deposition in the Extrathoracic Region. Aerosol Sci Technol. 2003; 37:659–671. [PubMed: 19011693]

Chew NYK, Chan H-K, Bagster DF, Mukhraiya J. Characterization of pharmaceutical powder inhalers: estimation of energy input for powder dispersion and effect of capsule device configuration. J Aerosol Sci. 2002; 33:999–1008.

Coates MS, Chan HK, Fletcher DF, Chiou H. Influence of mouthpiece geometry on the aerosol delivery performance of a dry powder inhaler. Pharm Res. 2007; 24:1450–1456. [PubMed: 17404813]

Coates MS, Fletcher DF, Chan HK, Raper JA. Effect of design on the performance of a dry powder inhaler using computational fluid dynamics. Part 1: Grid structure and mouthpiece length. J Pharm Sci. 2004; 93:2863–2876. [PubMed: 15389665]

Coates MS, Fletcher DF, Chan HK, Raper JA. The role of capsule on the performance of a dry powder inhaler using computational and experimental analyses. Pharm Res. 2005; 22:923–932. [PubMed: 15948036]

DeHaan WH, Finlay WH. Predicting extrathoracic deposition from dry powder inhalers. J Aerosol Sci. 2004; 35:309–331.

Delvadia RR, Longest PW, Byron PR. In vitro tests for aerosol deposition. I: Scaling a physical model of the upper airways to predict drug deposition variation in normal humans. J Aerosol Med Pulm Drug Deliv. 2012; 25:32–40. [PubMed: 22070526]

Dolovich M. New propellant-free technologies under investigation. J Aerosol Med. 1999; 12(Suppl 1):S9–S17. [PubMed: 10623341]

Fenton C, Keating GM, Plosker GL. Novolizer: a multidose dry powder inhaler. Drugs. 2003; 63:2437–2445. discussion 2447-2438. [PubMed: 14609355]

Ferron GA. The size of soluable aerosol particles as a function of the humidity of the air: Application to the human respiratory tract. J Aerosol Sci. 1977; 3:251–267.

Ferron GA, Kreyling WG, Haider B. Inhalation of salt aerosol particles - II. Growth and deposition in the human respiratory tract. J Aerosol Sci. 1988; 19:611–631.

Finlay, WH. The Mechanics of Inhaled Pharmaceutical Aerosols. San Diego: Academic Press; 2001.

Geller DE, Weers J, Heuerding S. Development of an inhaled dry-powder formulation of tobramycin using PulmoSphere technology. J Aerosol Med Pulm Drug Deliv. 2011; 24:175–182. [PubMed: 21395432]

Grgic B, Finlay WH, Burnell PKP, Heenan AF. In vitro intersubject and intrasubject deposition measurements in realistic mouth–throat geometries. J Aerosol Sci. 2004; 35:1025–1040.

Harper NJ, Gray S, De Groot J, Parker JM, Sadrzadeh N, Schuler C, Schumacher JD, Seshadri S, Smith AE, Steeno GS, Stevenson CL, Taniere R, Wang M, Bennett DB. The design and performance of the exubera pulmonary insulin delivery system. Diabetes Technol Ther. 2007; 9(Suppl 1):S16–S27. [PubMed: 17563300]

Hindle M, Longest PW. Condensational growth of combination drug-excipient submicrometer particles for targeted high-efficiency pulmonary delivery: evaluation of formulation and delivery device. J Pharm Pharmacol. 2012; 64:1254–1263. [PubMed: 22881438]

Hinds, WC. Aerosol Technology: Properties, Behavior, and Measurement of Airborne Particles. New York: John Wiley and Sons; 1999.

Islam N, Cleary MJ. Developing an efficient and reliable dry powder inhaler for pulmonary drug delivery – A review for multidisciplinary researchers. Med Eng Physics. 2012; 34:409–427.

Islam N, Gladki E. Dry powder inhalers (DPIs)—A review of device reliability and innovation. Int J Pharm. 2008; 360:1–11. [PubMed: 18583072]

Jaques PA, Kim CS. Measurement of total lung deposition of inhaled ultrafine particles in healthy men and women. Inhal Toxicol. 2000; 12:715–731. [PubMed: 10880153]

Longest PW, Hindle M. Evaluation of the Respimat Soft Mist inhaler using a concurrent CFD and in vitro approach. J Aerosol Med Pulm Drug Del. 2009; 22:99–112.

Longest PW, Hindle M. CFD simulations of enhanced condensational growth (ECG) applied to respiratory drug delivery with comparisons to in vitro data. J Aerosol Sci. 2010; 41:805–820. [PubMed: 20835406]

Longest PW, Hindle M. Numerical Model to Characterize the Size Increase of Combination Drug and Hygroscopic Excipient Nanoparticle Aerosols. Aerosol Sci Technol. 2011; 45:884–899. [PubMed: 21804683]

Longest PW, Hindle M. Condensational growth of combination drug-excipient submicrometer particles: Comparison of CFD predictions with experimental results. Pharm Res. 2012; 29:707–721. [PubMed: 21948458]

Longest PW, Hindle M, Das Choudhuri S, Byron PR. Numerical simulations of capillary aerosol generation: CFD model development and comparisons with experimental data. Aerosol Sci Technol. 2007; 41:952–973.

Longest PW, Hindle M, Das Choudhuri S, Xi J. Comparison of ambient and spray aerosol deposition in a standard induction port and more realistic mouth-throat geometry. J Aerosol Sci. 2008; 39:572–591.

Longest PW, Son YJ, Holbrook L, Hindle M. Aerodynamic Factors Responsible for the Deaggregation of Carrier-Free Drug Powders to form Micrometer and Submicrometer Aerosols. Pharm Res. 2013

Longest PW, Tian G, Li X, Son YJ, Hindle M. Performance of Combination Drug and Hygroscopic Excipient Submicrometer Particles from a Softmist Inhaler in a Characteristic Model of the Airways. Ann Biomed Eng. 2012b

Longest PW, Tian G, Walenga RL, Hindle M. Comparing MDI and DPI aerosol deposition using in vitro experiments and a new stochastic individual path (SIP) model of the conducting airways. Pharm Res. 2012c

Longest PW, Vinchurkar S. Validating CFD predictions of respiratory aerosol deposition: effects of upstream transition and turbulence. J Biomechanics. 2007; 40:305–316.

Longest PW, Xi J. Condensational growth may contribute to the enhanced deposition of cigarette smoke particles in the upper respiratory tract. Aerosol Sci Technol. 2008; 42:579–602.

Newman SP, Busse WW. Evolution of dry powder inhaler design, formulation, and performance. Respir Med. 2002; 96:293–304. [PubMed: 12113378]

Newman SP, Pitcairn GR, Hirst PH, Bacon RE, O'Keefe E, Reiners M, Hermann R. Scintigraphic comparison of budesonide deposition from two dry powder inhalers. Eur Respir J. 2000; 16:178–183. [PubMed: 10933104]

Smith IJ, Parry-Billings M. The inhalers of the future? A review of dry powder devices on the market today. Pulm Pharmacol Ther. 2003; 16:79–95. [PubMed: 12670777]

Son Y-J, Longest PW, Hindle M. Aerosolization Characteristics of Dry Powder Inhaler Formulations for the Enhanced Excipient Growth (EEG) Application: Effect of Spray Drying Process Conditions on Aerosol Performance. Int J Pharm. 2013; 443(1):137–145. [PubMed: 23313343]

Son Y-J, Longest PW, Hindle M. Aerosolization characteristics of dry powder inhaler formulations for the enhanced excipient growth application: Effect of DPI design. Respiratory Drug Delivery 2012. 2012b; 3:903–906.

Son Y-J, Longest PW, Hindle M. Aerosolization characteristics of dry powder inhaler formulations for the enhanced excipient growth application: Effect of spray drying conditions. Respiratory Drug Delivery 2012. 2012c; 3:899–902.

Son Y-J, McConville JT. Advancements in Dry Powder Delivery to the Lung. Drug Dev Ind Pharm. 2008; 34:948–959. [PubMed: 18800256]

Srichana T, Martin GP, Marriott C. Dry powder inhalers: the influence of device resistance and powder formulation on drug and lactose deposition in vitro. Eur J Pharm Sci. 1998; 7:73–80. [PubMed: 9845780]

Sumby B, Slater A, Atkins PJ, Prime D. Review of dry powder inhalers. Adv Drug Deliv Rev. 1997; 26:51–58. [PubMed: 10837532]

Tian G, Longest PW, Li X, Hindle M. Targeting Aerosol Deposition to and within the Lung Airways using Excipient Enhanced Growth. J Aerosol Med Pulm Drug Del. 2012

Tian G, Longest PW, Su G, Hindle M. Characterization of respiratory drug delivery with enhanced condensational growth using an individual path model of the entire tracheobronchial airways. Ann Biomed Eng. 2011a; 39:1136–1153. [PubMed: 21152983]

Tian G, Longest PW, Su G, Walenga RL, Hindle M. Development of a stochastic individual path (SIP) model for predicting the tracheobronchial deposition of pharmaceutical aerosols: Effects of transient inhalation and sampling the airways. J Aerosol Sci. 2011b; 42:781–799.

Timsina MP, Martin GP, Marriott C, Ganderton D, Yianneskis M. Drug delivery to the respiratory tract using dry powder inhalers. Int J Pharm. 1994; 101:1–13.

Vinchurkar S, Longest PW. Evaluation of hexahedral, prismatic and hybrid mesh styles for simulating respiratory aerosol dynamics. Computers and Fluids. 2008; 37:317–331.

Voss A, Finlay WH. Deagglomeration of dry powder pharmaceutical aerosols. Int J Pharm. 2002; 248:39–50. [PubMed: 12429458]

Xi J, Longest P. Transport and Deposition of Micro-Aerosols in Realistic and Simplified Models of the Oral Airway. Ann Biomed Eng. 2007; 35:560–581. [PubMed: 17237991]

Xi J, Longest PW. Effects of oral airway geometry characteristics on the diffusional deposition of inhaled nanoparticles. J Biomech Eng. 2008; 130:011008. [PubMed: 18298184]

Xi J, Longest PW, Martonen TB. Effects of the laryngeal jet on nano- and microparticle transport and deposition in an approximate model of the upper tracheobronchial airways. J App Physiol. 2008; 104:1761–1777.

Yang W, Peters JI, Williams RO. Inhaled nanoparticles—A current review. Int J Pharm. 2008; 356:239–247. [PubMed: 18358652]

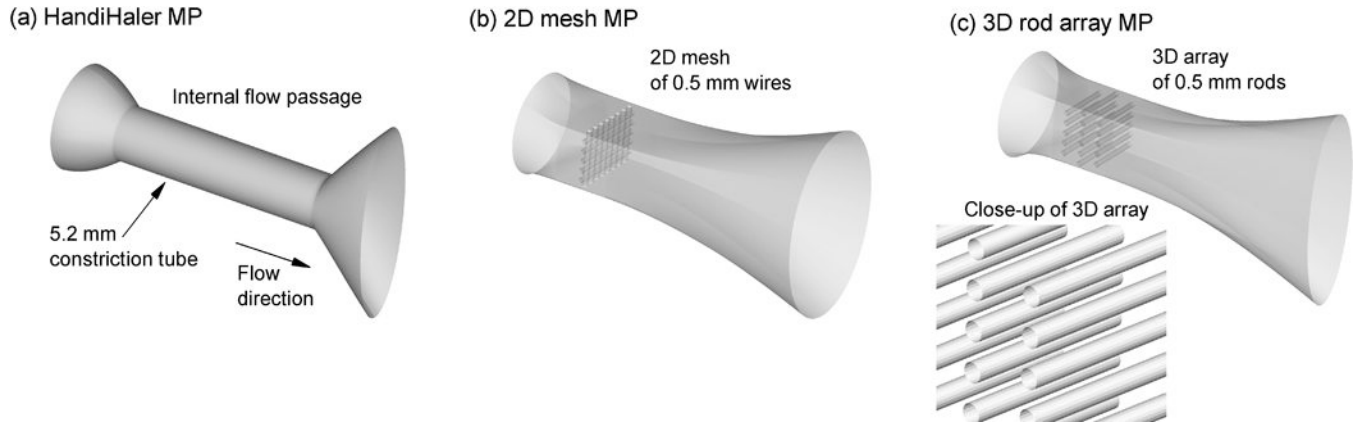

Figure 1.
Mouthpiece (MP) flow passage design: (a) HandiHaler, (b) 2D-mesh (HH-2D), and (c) 3D array of rods (HH-3D).

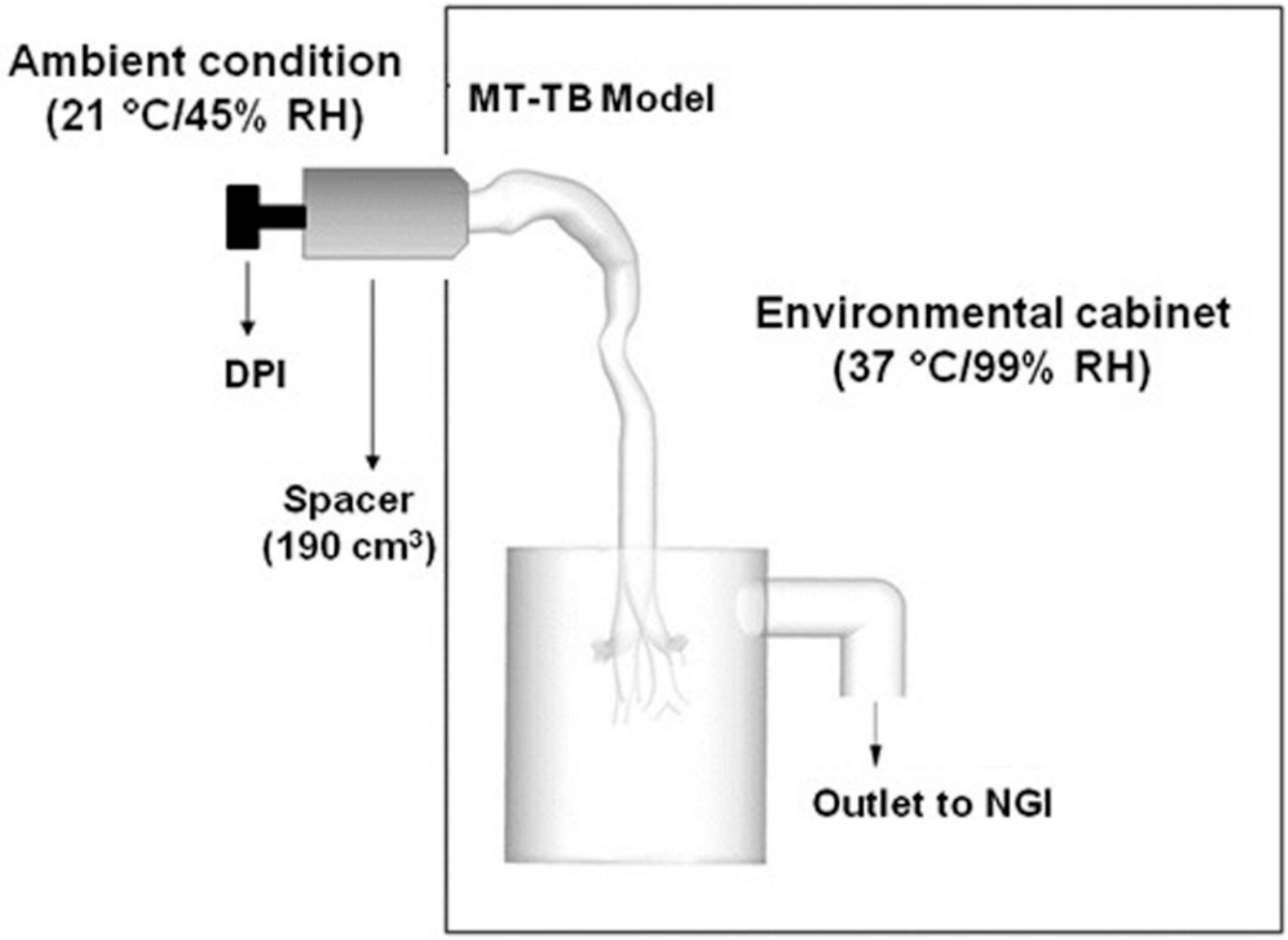

Figure 2.
Schematic diagram of experimental setup for evaluating the hygroscopic growth of combination particle aerosols using simulated airway conditions.

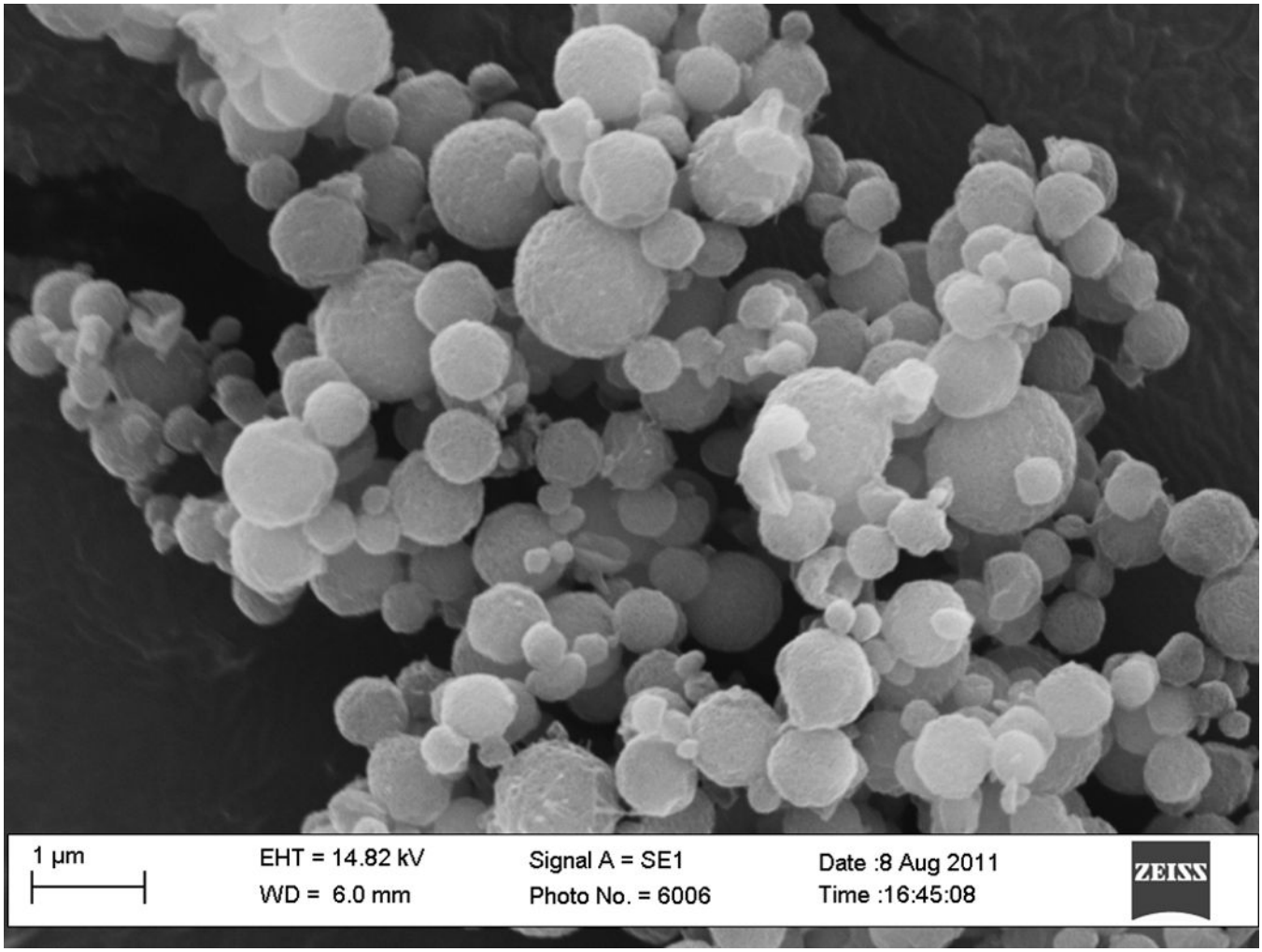

Figure 3.
Scanning electron micrograph of the excipient enhanced growth submicrometer spray dried formulation

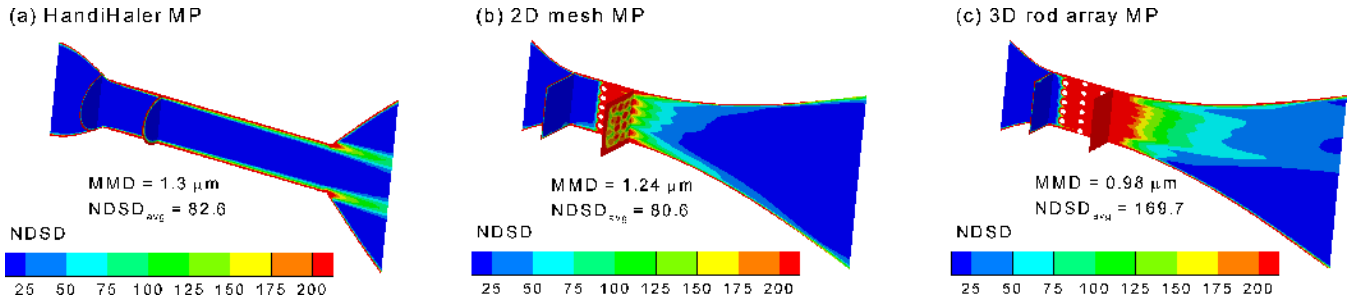

Figure 4.

Non-dimensional specific dissipation (NDSD), which correlates with deaggregation of the aerosol and reduced MMDs, for the (a) HandiHaler MP, (b) 2D mesh MP, and (c) 3D rod array MP at flow rates of 45, 53, and 45 L/min, respectively.

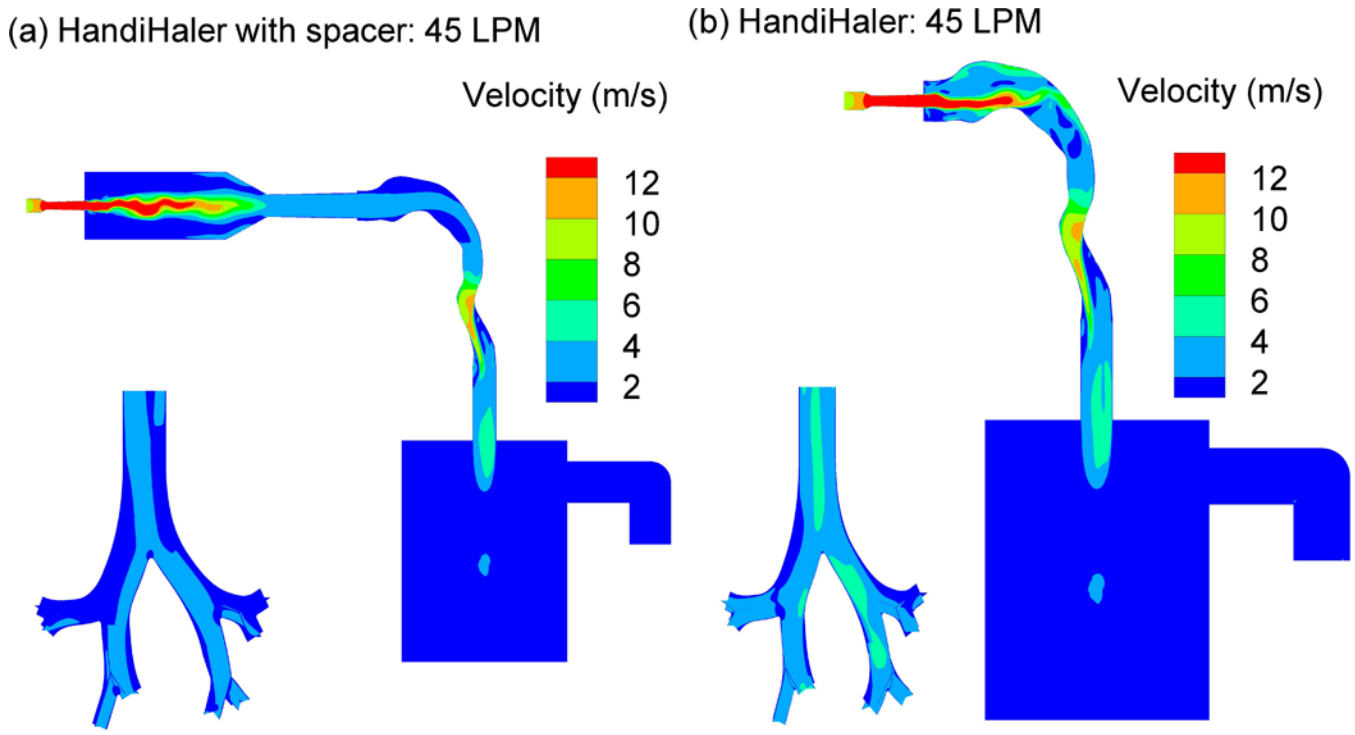

Figure 5.
Velocity profiles for EEG aerosols generated at 45 L/min into the MT-TB experimental setup using the HandiHaler (a) with and (b) without the spacer.

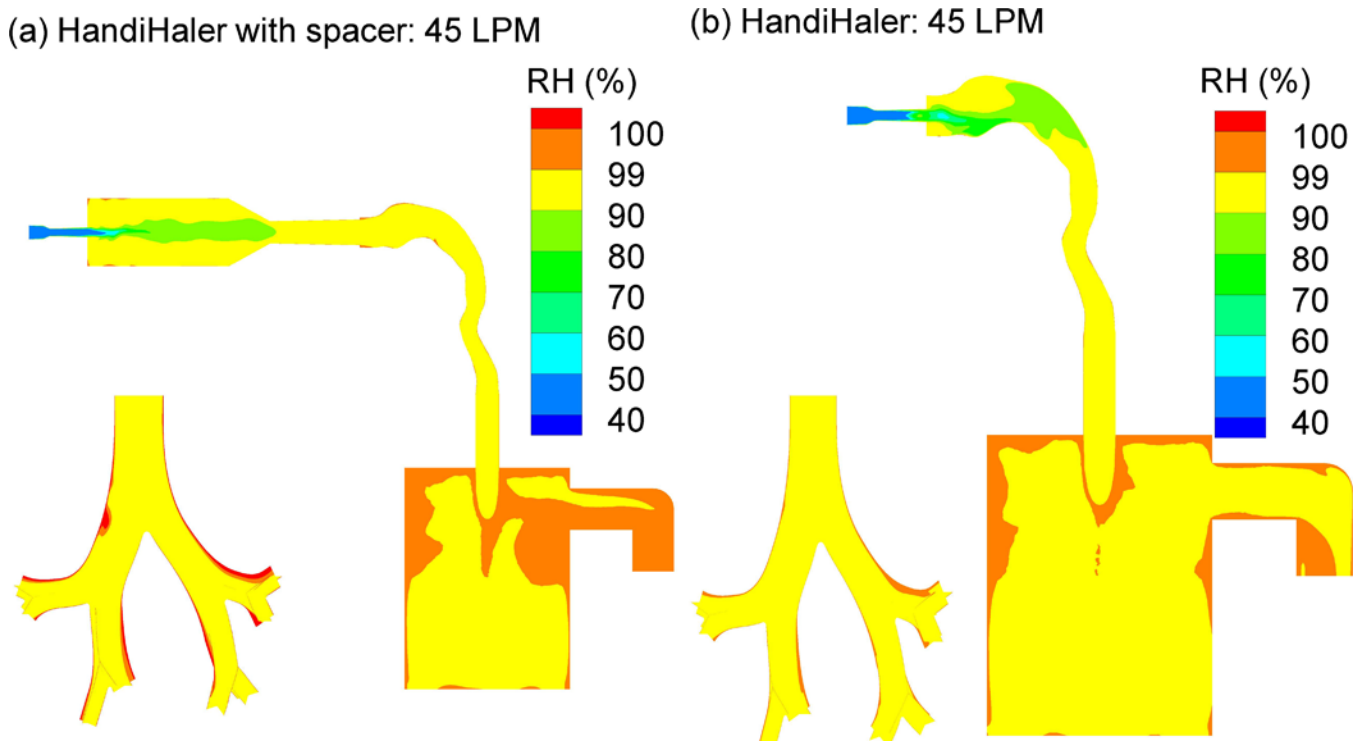

Figure 6.
Relative humidity (RH) contours for EEG aerosols generated at 45 L/min into the MT-TB experimental setup using the HandiHaler (a) with and (b) without the spacer.

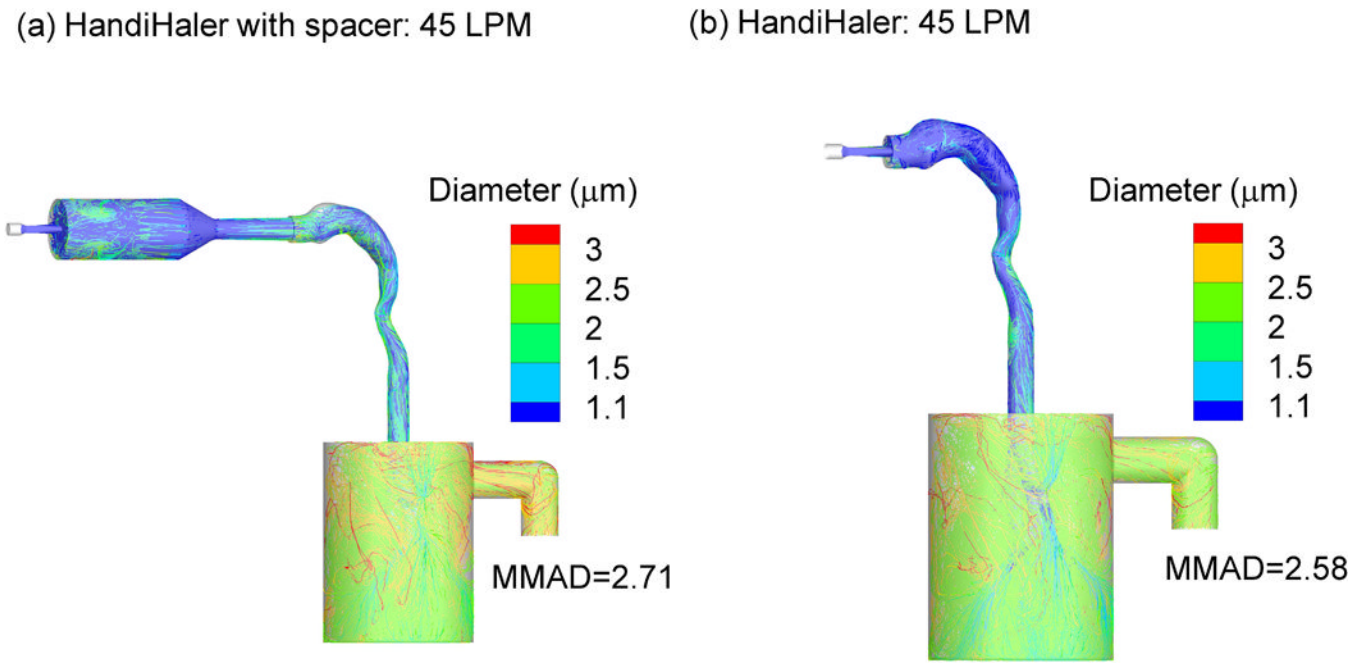

Figure 7.
Particle growth trajectories and final growth sizes for EEG aerosols generated at 45 L/min into the MT-TB experimental setup using the HandiHaler (a) with and (b) without the spacer.

Table 1

Aerosol performance of the combination EEG formulation following aerosolization using conventional DPIs (values are means and SD in parenthesis, n = 3).

Device	Dosing	Flow rate (L/min)	ED (%)*	$FPF_{5\mu m/ED}$ (%)*	$FPF_{1\mu m/ED}$ (%)*	MMAD (μm)*	MMD (μm)‡
Active DPIs							
Exubera	Blister	30	62.8 (3.1)	96.3 (0.7)	9.6 (0.5)	2.0 (0.0)	1.7
Spiros	Blister	30	73.7 (4.1)	80.2 (3.1)	6.8 (0.6)	2.6 (0.1)	2.2
Passive DPIs							
Novolizer	Reservoir	80	82.4 (3.7)	91.3 (2.9)	11.0 (2.6)	2.0 (0.2)	1.7
HandiHaler	Capsule	45	78.2 (2.7)	87.6 (3.6)	19.5 (3.1)	1.6 (0.1)	1.4
Aerolizer	Capsule	80	81.4 (2.0)	95.3 (1.1)	28.3 (3.1)	1.4 (0.1)	1.2

*Statistically significant effects of DPI devices on the aerosolization properties of EEG formulation: ED, $FPF_{5\mu m/ED}$ and $FPF_{1\mu m/ED}$ and MMAD; one-way ANOVA, $P < 0.05$

‡The mass median diameter (MMD) of aerosol was derived from the MMAD and skeletal density (ρ= 1.33 g/cm^3), according to the following equation: $MMAD = MMD \times \sqrt{\rho}$

Eur J Pharm Sci. Author manuscript; available in PMC 2014 June 14.

Table 2

The aerodynamic characteristics of EEG combination particles aerosolized using modified HandiHalers (values are means and SD in parenthesis, n = 3).

Modification	Capsule piercing	Hole size (mm)	ED (%)*	MMAD (μm)*	$FPF_{5\mu m/ED}$ (%)*	$FPF_{1\mu m/ED}$ (%)*	MMD (μm)	NDSD
HandiHaler (HH)	HH	1.5	78.2 (2.7)	1.6 (0.1)	87.6 (3.6)	19.5 (3.1)	1.40	82.6
HH-Cap	Needle	0.5	78.9 (3.1)	1.5 (0.0)	94.6 (1.1)	24.5 (0.5)	1.30	NA
HH-2D	Needle	0.5	81.2 (0.9)	1.4 (0.0)	97.2 (0.9)	24.1 (3.2)	1.24	80.6
HH-3D	Needle	0.5	74.2 (1.4)	1.1 (0.1)	97.3 (0.3)	38.8 (6.3)	0.98	169.7

*Statistically significant effects of DPI devices on the aerosolization properties of EEG formulation: ED, $FPF_{5\mu m/ED}$ and $FPF_{1\mu m/ED}$ and MMAD; one-way ANOVA, $P < 0.05$

Table 3

The mean (SD in parenthesis) AS deposition and aerosol growth characteristics of the EEG formulation aerosolized using the HH-3D at a flow rate of 45 L/min ($n \geq 4$) into the MT-TB airway geometry experimental setup (Figure 2).

	Simulated airway conditions (37°C/99% RH)
MT (%)	2.6 (1.5)
TB (%)	2.1 (0.4)
Final MMAD (μm)	2.8 (0.1)
$FPF_{5\mu m/ED}$ (%)	75.5 (2.7)
$FPF_{1\mu m/ED}$ (%)	3.0 (0.5)